Int. J. Radiation Oncology Biol. Phys., Vol. ■, No. ■, pp. 1–8, 2011

0360-3016/$ - see front matter

ELSEVIER

doi:10.1016/j.ijrobp.2011.01.068

CLINICAL INVESTIGATION

DIFFUSION TENSOR IMAGING OF NORMAL-APPEARING WHITE MATTER AS BIOMARKER FOR RADIATION-INDUCED LATE DELAYED COGNITIVE DECLINE

Christopher H. Chapman, B.A.,* Vijaya Nagesh, Ph.D.,* Pia C. Sundgren, M.D., Ph.D.,†‡ Henry Buchtel, Ph.D.,§¶ Thomas L. Chenevert, Ph.D.,† Larry Junck, M.D.,‖ Theodore S. Lawrence, M.D., Ph.D.,* Christina I. Tsien, M.D.,* and Yue Cao, Ph.D.*†

Departments of *Radiation Oncology, †Radiology, §Psychiatry, and ‖Neurology, University of Michigan Medical School, Ann Arbor, MI; ‡Department of Radiology, Skåne University Hospital, Lund, Sweden; ¶Veterans Affairs Ann Arbor Healthcare System, Ann Arbor, MI

Purpose: To determine whether early assessment of cerebral white matter degradation can predict late delayed cognitive decline after radiotherapy (RT).

Methods and Materials: Ten patients undergoing conformal fractionated brain RT participated in a prospective diffusion tensor magnetic resonance imaging study. Magnetic resonance imaging studies were acquired before RT, at 3 and 6 weeks during RT, and 10, 30, and 78 weeks after starting RT. The diffusivity variables in the parahippocampal cingulum bundle and temporal lobe white matter were computed. A quality-of-life survey and neurocognitive function tests were administered before and after RT at the magnetic resonance imaging follow-up visits.

Results: In both structures, longitudinal diffusivity ($\lambda_{||}$) decreased and perpendicular diffusivity ($\lambda_{\perp}$) increased after RT, with early changes correlating to later changes ($p < .05$). The radiation dose correlated with an increase in cingulum $\lambda_{\perp}$ at 3 weeks, and patients with >50% of cingula volume receiving >12 Gy had a greater increase in $\lambda_{\perp}$ at 3 and 6 weeks ($p < .05$). The post-RT changes in verbal recall scores correlated linearly with the late changes in cingulum $\lambda_{||}$ (30 weeks, $p < .02$). Using receiver operating characteristic curves, early cingulum $\lambda_{||}$ changes predicted for post-RT changes in verbal recall scores (3 and 6 weeks, $p < .05$). The neurocognitive test scores correlated significantly with the quality-of-life survey results.

Conclusions: The correlation between early diffusivity changes in the parahippocampal cingulum and the late decline in verbal recall suggests that diffusion tensor imaging might be useful as a biomarker for predicting late delayed cognitive decline.

Diffusion tensor imaging, Neurocognitive function, Late-delayed effects, Biomarker, Quality of life.

INTRODUCTION

A limitation of radiotherapy (RT) for cranial tumors is the toxicity to the central nervous system. Radiation-induced brain injury has traditionally been divided into three temporal phases: acute, early delayed, and late delayed. Although acute and early delayed effects are transient, late delayed injury is usually permanent and is characterized by necrosis and histopathologic abnormalities. Severe late delayed effects are typically seen ≥6 months after RT and at doses >60 Gy (1). However, permanent late delayed cognitive deterioration can occur at doses <60 Gy. This late delayed cognitive decline is observed without necrosis or lesions visible on T_1- and T_2-weighted magnetic resonance imaging (MRI) (2). It has been psychologically characterized as declines in short-term memory, attention, and executive function (3). The effect of late delayed cognitive decline on quality of life has become increasingly important as the survival times have lengthened (4). Chang *et al.* (5) have demonstrated that the risk of neurocognitive decline in patients receiving whole-brain RT and stereotactic RT is greater than in those receiving stereotactic RT alone; therefore, early tissue biomarkers of neurocognitive decline would be beneficial for guiding RT delivery and improving outcomes.

Our understanding of what causes late delayed cognitive decline is still limited. Traditional theories have considered radiation-induced encephalopathy to be exclusively a result

Reprint requests to: Christopher H. Chapman, B.A. , Department of Radiation Oncology, University of Michigan Medical School, 519 W. William St., Argus Bldg. 1, Ann Arbor, MI 48103-4943. Tel: (734) 647-4436; Fax: (734) 936-7859; E-mail: chchap@umich.edu

Presented at the First Biennial Meeting for Imaging and Treatment Assessment in Radiation Therapy (ITART), June 21–22, 2010, National Harbor, MD.

Supported by National Institutes of Health Grants RO1 NS064973 and 3 PO1 CA59827.

Conflict of interest: none.

Acknowledgments—The authors thank Kristin Brierley for research study coordination, Dan Tatro for dosimetry assistance, and Zhou Shen for computer software support.

Received Sept 1, 2010, and in revised form Jan 7, 2011. Accepted for publication Jan 31, 2011.

of damage to cells of either oligodendrocyte or vascular endothelium lineage (1). Accumulating evidence has now indicated that a single target of radiation is unlikely, and that astrocytes, microglia, neurons, and neural stem cells are also involved in a long-term, multifactorial, and dynamic process (1, 6). However, as a proximal cause of late neurocognitive dysfunction, white matter damage as manifested by demyelination and axonal degradation most likely plays a role. In 2001, Akiyama *et al.* (7) observed demyelination in a rat model of radiation-induced late delayed neurocognitive decline. In humans, numerous cross-sectional studies have correlated white matter degradation with cognitive decline in adult survivors of childhood cancers (8–10). However, these studies were retrospective and were performed years after treatment. A prospective longitudinal study would be better able to address how white matter changes after brain RT and whether the changes correlate with late delayed cognitive decline.

One of the best methods for evaluating white matter degradation is diffusion tensor MRI (DTI). DTI makes use of the fact that within the brain, water molecules preferentially move along the long axis of myelinated fiber bundles, leading to unequal diffusion (anisotropy) in that direction. By quantifying the magnetic resonance signal of the water molecule motion in multiple directions, DTI produces a three-dimensional image of the diffusivity characteristics of the brain. DTI has been shown to be more sensitive than T_1- and T_2-weighted MRI for detecting subtle white matter damage (11). We anticipated that DTI might be able to detect the white matter degradation associated with late delayed cognitive decline not visible using traditional MRI modalities.

Few studies have used DTI to investigate the effects of radiation on the human brain longitudinally. In 2008, Haris *et al.* (12) published longitudinal data showing decreased anisotropy in higher dose areas of subcortical white matter. Our previous study tracked DTI changes in the corpus callosum of 25 patients, showing significant and dose-dependent changes in diffusivity as early as 4 weeks after finishing RT (13). However, these previous longitudinal studies did not examine the functional consequences of radiation-induced white matter damage. Both evaluated white matter structures chosen for ease of contouring, and neither measured neurocognitive function, leaving the link between white matter damage and functional impairment incomplete.

The purpose of the present study was to examine the connection between white matter degradation and radiation-induced late delayed cognitive decline. We hypothesized that early radiation-induced changes in white matter integrity would progress into more advanced white matter degradation and cause late delayed cognitive decline; thus, early DTI changes could be used as a biomarker for late delayed neurotoxicity. To test this hypothesis, we performed serial DTI and neurocognitive tests on patients before and after RT. We addressed three questions: *(1)* how the DTI characteristics of normal-appearing white matter change after RT; *(2)* how these changes are related to the radiation dose; and *(3)* whether these changes correlated with neurocognitive function.

METHODS AND MATERIALS

Study design

A total of 10 patients with low-grade or benign tumors were enrolled in a prospective, institutional review board-approved, clinical MRI study. All patients underwent a standard, 6-week course of daily fractionated conformal cranial RT, with a median dose of 54 Gy to 95% of the planning target volume (Table 1). Overall function was assessed before RT using the Karnofsky performance status scale (KPS), the Folstein Mini-Mental State Examination (MMSE), and Radiation Therapy Oncology Group neurologic function class. All patients had a KPS score of $\geq$80, MMSE score of $\geq$27, and neurologic function class of 1 or 2, indicating high overall function. The KPS, MMSE, and neurologic function class were also assessed at each scan point after RT.

Ethical guidelines

The University of Michigan Medical School institutional review board prospectively approved the present study. Data and safety monitoring were performed by the University of Michigan Radiation Oncology Department and reported to the University of Michigan Comprehensive Cancer Center Data and Safety Monitoring Board. Patient confidentiality was maintained during all phases of the study.

Diffusion tensor MRI

Patients underwent an MRI scan at 6 points: 1–2 weeks before RT, 3 weeks into RT, 6 weeks into RT (end of RT), and 10, 30,

Table 1. Patient characteristics

Pt. No.	Age (y)/gender	Diagnosis	Location	Prescribed dose (Gy)/fractions (*n*)
1	33/Male	Grade 2 gemistocytic astrocytoma	Right temporal	59.4/33
2	64/Male	Pituitary macroadenoma	Suprasellar	50.4/28
3	55/Male	Sphenoid wing meningioma	Left medial sphenoid	54.0/30
4	29/Male	Cranopharyngioma	Suprasellar	55.8/31
5	25/Female	Low grade glioma	Left frontal	54.0/30
6	71/Male	Null cell pituitary adenoma	Suprasellar	50.4/28
7	36/Male	WHO III anaplastic supratentorial ependymoma	Left frontal	59.4/33
8	55/Male	Grade 2 astrocytoma	Bifrontal	54.0/30
9	39/Male	Grade 2 mixed oligoastrocytoma	Right frontotemporal	59.4/33
10	44/Male	Pituitary macroadenoma	Suprasellar	50.4/28

Abbreviations: Pt. No. = patient number; WHO = world health organization.

and 78 weeks after starting RT. All MRI scans were done using a 1.5T scanner (GE Healthcare, Milwaukee, WI). The MRI series included T_1- and T_2-weighted images, DTI, and postcontrast T_1-weighted images. DTI was acquired using a spin-echo echo-planar imaging sequence with a repetition time of 10,000 ms, echo time of 70 ms, 360 mm^2 field of view, 128 × 128 matrix, and 4-mm slice thickness, with a 0-mm gap. For each axial slice, the diffusion-sensitizing gradient encoding with a diffusion weighting factor of b = 1,000 s/mm^2 was applied in nine noncolinear directions, and one set of null images with b = 0 s/mm^2 was acquired.

Image registration and processing

The diffusion tensor images were co-registered to the postcontrast T_1-weighted image set acquired before RT. The diffusion-weighted images were registered using mutual information and affine transformation, which included 12 parameters (9 for 3 × 3 rotation and shearing matrix and 3 for translation). Similarly, the treatment planning computed tomography scan and spatially distributed radiation dose maps were co-registered to the postcontrast T_1-weighted image set acquired before RT.

DTI analysis

DTI was used to assess the structural changes in the white matter fiber tracts. Several diffusion indexes can be calculated from the diffusion tensor. Two commonly reported indexes are the trace diffusivity (Dtr) and the fractional anisotropy of diffusion (FA). Dtr, the sum of the diffusivities in three orthogonal directions, is an orientation-independent measure of the total displacement of water molecules. FA is a unitless index that measures the degree of anisotropic diffusion. The FA values are between 0 and 1, with a greater value denoting greater anisotropy. Additional information can be provided by eigen-diffusivities (λ_1, λ_2, and λ_3) along the three principal directions (14). In the brain, the largest eigen-diffusivity, λ_1, represents water diffusion along the direction parallel to the axonal fibers, hereafter labeled $\lambda_{||}$, which is sensitive to axonal injury and astrogliosis but not demyelination (15, 16). The λ_2 and λ_3 components denote diffusivities in the two orthogonal directions perpendicular to the axonal fibers. The mean of λ_2 and λ_3 is termed $\lambda_\perp$, which is sensitive to demyelination (15, 17). Maps of Dtr, FA, $\lambda_{||}$, and $\lambda_\perp$ were calculated using Functional Imaging Analysis Tool (FIAT), an imaging software package developed in-house (18).

Volumes of interest

Normal-appearing white matter (*i.e.*, tissue that appeared normal on T_1- and T_2-weighted MRI scans) was studied in the parahippocampal cingulum bundle and the subcortical temporal lobe white matter. Diffusivity differences in these structures have previously been associated with cognitive impairment (19, 20). The volumes of interest were contoured on multiple axial levels using a combination of T_1-weighted and FA images acquired before RT (Fig. 1). Hippocampal gray matter was contoured first (not used for the DTI indexes). The parahippocampal cingulum bundle was defined as cingulum white matter at the same axial levels as the hippocampus with a pre-RT FA value of ≥0.250, a value chosen as a reasonable lower bound for white matter structures according to previous experience (13). Temporal lobe white matter was contoured at the same axial levels with the assistance of autosegmentation in FIAT. The volumes were copied onto pre-RT T_2-weighted images and edited to exclude any tumor or peritumoral edematous tissue. The volumes were then transferred to co-registered images from later points and linearly translated to ensure good fit over the structures of interest and maximizing the mean contour FA. Because the FA was used for volume adjustment, it was not included in the analysis.

The mean values of $\lambda_{||}$, $\lambda_\perp$, and Dtr were obtained for each structure at each point from the DTI maps. The primary outcomes evaluated were the percentage of change in the diffusivity indexes from before RT to the later points.

The fraction of volume receiving ≥12 Gy ($\%V_{12}$) and mean dose (volume-weighted average dose) to each structure was also obtained from the co-registered radiation dose map. $\%V_{12}$ was chosen because of the Quantitative Analysis of Normal Tissue Effects in

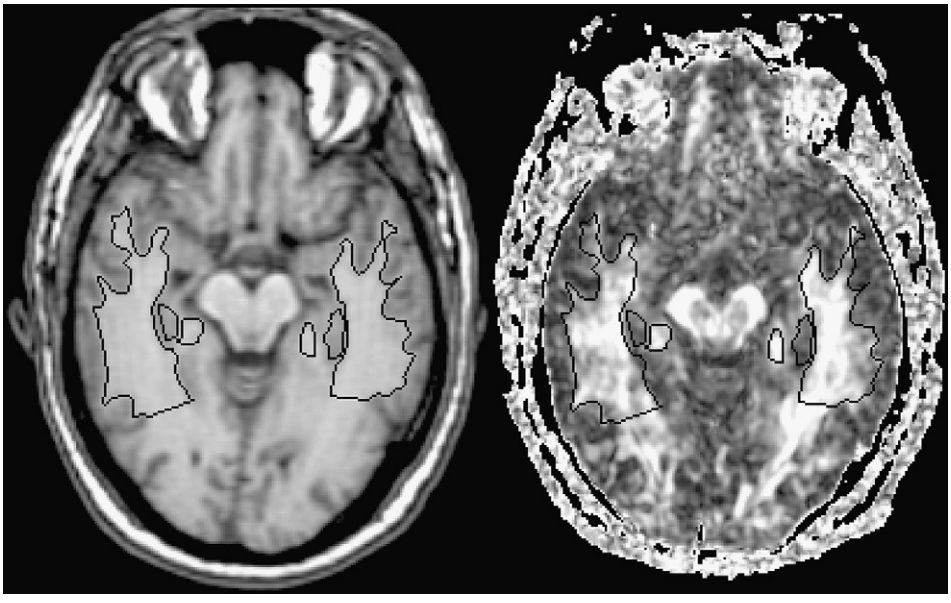

Fig. 1. Example of volume locations from Patient 10. (Left) Axial preradiotherapy T_1-weighted image. (Right) Axial preradiotherapy fractional anisotropy of diffusion image (white indicates high anisotropy). Volumes outlined in black. Medial to lateral: parahippocampal cingulum bundle, hippocampal gray matter, temporal lobe white matter.

Table 2. Quality-of-life survey correlation to neurocognitive test scores

QOL	HVLT-TR	HVLT-DR	COWA	TMT
Total	.021*	.091	.079	.002*
Cognitive	.009†	.012	.019	.037

Abbreviations: QOL = quality of life; HVLT = hopkins verbal learning test; TR = total recall; DR = delayed recall; COWA = controlled oral word association; TMT = trail making test B – trail making test A; EORTC = european organization for research and treatment of cancer.

Data presented as p values by Pearson's product-moment correlation.

Cognitive QOL questions.

During the past week:

Have you had difficulty concentrating on things, like reading a newspaper or watching television?

Have you had difficulty remembering things?

Did you have trouble finding the right words to express yourself?

Did you have difficulty speaking?

Did you have trouble communicating your thoughts?

Total score on EORTC QLQ-C30 and EORTC QLQ-BN20 correlated with neurocognitive test scores (total QOL); scores for 5 questions related to cognitive performance retrospectively chosen for correlation to neurocognitive test scores (cognitive QOL).

* Significant correlation ($p < .05$).

† Significant correlation, post hoc threshold ($p < .01$).

the Clinic (QUANTEC) recommended use in normal tissue dose limits for radiosurgery (21). The linear-quadratic model was applied on a voxel-by-voxel basis to find the biologically corrected dose using an α/β ratio of 2.50 (22). Hereafter, the biologically corrected doses will be referred to as "dose."

Neurocognitive function tests

All patients underwent standardized neurocognitive function tests before RT and at the post-RT follow-up examinations. The tests included the Hopkins Verbal Learning Test (HVLT) (verbal recall), Controlled Oral Word Association Test (verbal fluency), and Trail Making Tests A and B (executive function) (3).

Late delayed cognitive decline was defined as the difference between the score at 78 weeks and the post-RT maximal score (at 10 or 30 weeks). Previously published data have shown that the average intrasubject test–retest variability of these neurocognitive tests is approximately ±0.25 times the age-matched standard deviation. (23–25). Therefore, a decline in neurocognitive test score >0.5 times the age-matched standard deviation was considered neurocognitive decline. This is similar to the thresholds used in previous large clinical trials (5, 26).

Along with the neurologic function tests, two standardized quality-of-life questionnaires (European Organization for Research and Treatment of Cancer [EORTC] QLQ-C30 and EORTC QLQ-BN20) (27, 28) were administered before RT and on the same days as the post-RT MRI scans. After the quality-of-life results were correlated with the neurocognitive test scores, five questions related to self-assessment of cognitive performance were chosen retrospectively for additional comparison with the neurocognitive test scores (Table 2). Because of its post hoc nature, the latter comparison was considered significant at $p < .01$.

Statistical analysis

Statistical analysis was performed using the Statistical Package for Social Sciences (SPSS Software Products, Chicago, IL). A pairwise two-tailed Student's t test was used to evaluate differences between the volumes and across the follow-up points. Associations among the DTI indexes, time of MRI scan, cognitive test scores, and radiation dose were evaluated using Pearson's product-moment correlation. Receiver operating characteristic curve analysis was used to evaluate the predictive value of DTI changes, age, and radiation dose on cognitive test scores. The results of statistical tests were considered statistically significant at $p < .05$.

RESULTS

Clinical and radiologic findings

None of the patients had exhibited tumor progression by 30 weeks after the start of RT. Patient 8 developed progression after 30 weeks and did not contribute DTI data after that point. No patient showed radiation-induced lesions on T_2-weighted or pre- and postgadolinium-enhanced T_1-weighted images at ≤78 weeks. No interval changes were noted in the tumors or tumor-related hyperintensities. All patients maintained a KPS score of ≥80, MMSE score of ≥26, and Radiation Therapy Oncology Group neurologic function class of 1 or 2, indicating that major neurologic function was preserved.

Dose delivery

The mean $\%V_{12}$ and average mean dose to contoured structures across all patients are reported in Table 3. No significant difference was found between the left and right hemisphere doses among the paired structures.

Temporal changes in DTI characteristics

Decreases in longitudinal diffusivity ($\lambda_{||}$) and increases in perpendicular diffusivity ($\lambda_{\perp}$) from the pre-RT values were observed in the cingula and temporal lobe white matter beginning 3 weeks after starting RT and remaining until 78 weeks after, indicating white matter degradation (Table 4

Table 3. Dose delivery: mean dose and fraction of volume receiving ≥12 Gy

Structure	Mean dose (Gy)	Range (Gy)	SD (Gy)	Mean $\%V_{12}$ (%)	Range (%)	SD (%)
Left hippocampus	32.7	16.0–54.7	15.3	87.6	52.5–100	19.3
Right hippocampus	30.0	11.5–55.5	15.2	84.8	43.3–100	23.8
Left cingulum	26.6	9.13–50.9	16.1	73.4	20.2–100	35.3
Right cingulum	25.7	8.60–55.8	16.7	72.4	9.10–100	37.1
Left temporal lobe	21.2	8.81–42.9	14.3	60.6	12.8–100	34.5
Right temporal lobe	21.1	7.28–55.5	18.3	56.3	4.44–100	34.1

Abbreviations: SD = standard deviation; $\%V_{12}$ = fraction of volume receiving ≥12 Gy.

Table 4. Diffusion tensor magnetic resonance imaging indexes

		During RT		After RT		
DTI index	Before RT	3 wk	6 wk	10 wk	30 wk	78 wk
Cingula $\lambda_{\|\|}$	1,196 ± 24	1,167 ± 18	1,170 ± 18	1,167 ± 24*	1,142 ± 12*	1,133 ± 30*
Cingula $\lambda_{\perp}$	699 ± 9	719 ± 11	722 ± 12*	735 ± 16*	750 ± 12*	744 ± 13*
Temporal $\lambda_{\|\|}$	1,073 ± 12	1,061 ± 13	1,054 ± 12	1,058 ± 13	1,047 ± 9*	1,040 ± 17
Temporal $\lambda_{\perp}$	676 ± 8	675 ± 6	678 ± 8	677 ± 7	687 ± 7	691 ± 7*

Abbreviations: DTI = diffusion tensor magnetic resonance imaging; RT = radiotherapy.
Data presented as mean ± standard error in units of $10^{-6} \times mm^2/s$.
* Significantly different ($p < .05$) from before RT by pairwise *t* test.

and Fig. 2). Changes in Dtr from before RT were never more than ±2% and were not significant at any point in any structure.

In the cingula, the increase in $\lambda_{\perp}$ compared with the pre-RT values was significant on the MRI scans 6 weeks after the start of RT and later, and the decrease in $\lambda_{||}$ was significant on the MRI scans 10 weeks after RT and later. By 78 weeks, the mean $\lambda_{||}$ in the cingula had decreased 4.8% and the mean $\lambda_{\perp}$ had increased 6.6%. Additionally, the percentage of change in the cingula $\lambda_{||}$ at 6 weeks after starting RT correlated positively with the percentage of decrease in cingula $\lambda_{||}$ at 30 weeks after starting RT, indicating that early changes predicted the late changes (R = 0.698, $p < .05$; Fig. 3).

In the temporal lobe, the magnitude of the changes was smaller than that in the cingula; by 78 weeks after the start of RT, the mean $\lambda_{||}$ in the temporal lobe had decreased 2.4% and mean $\lambda_{\perp}$ had increased 2.8%. The temporal lobe changes in $\lambda_{||}$ and $\lambda_{\perp}$ were significant at 30 and 78 weeks, respectively, after starting RT.

Dose dependency

We evaluated the effect of radiation dose on the white matter structures on changes in $\lambda_{||}$ and $\lambda_{\perp}$ after beginning RT. We found that the mean dose to the cingula correlated positively with the increase in $\lambda_{\perp}$ at 3 weeks into RT, when approximately one-half of the prescribed radiation dose had been received (R = 0.493, $p < .05$; Fig. 4). By 6 weeks after starting RT, the trend remained, but the correlation was not significant (R = 0.376, $p = .12$). At 3 and 6 weeks into RT, the patients with a cingula $\%V_{12}$ >50% had an average increase in $\lambda_{\perp}$ of 5.3% and 6.0%, respectively. Those with a cingula $\%V_{12}$ <50% had little change in $\lambda_{\perp}$ ($p < .03$, Fig. 5). We found no significant correlation between the mean dose and changes in the cingulum $\lambda_{||}$ or temporal lobe white matter diffusivity.

Neurocognitive function changes

The mean post-RT Z-score changes on the neurocognitive function tests are displayed in Table 5. On average, 33% of patients exhibited neurocognitive decline, a proportion very similar to that found in previous large clinical trials of brain RT (5, 26). Because of tumor progression, Patient 8 was not included in the neurocognitive function analyses. To check for confounding correlations, we confirmed that age did not significantly correlate with the Z-score change after RT.

The diffusivity index changes correlated with the neurocognitive test results. Using Pearson's product-moment correlation, changes in the cingula $\lambda_{||}$ at 30 weeks were significantly correlated with the post-RT Z-score change in the HVLT–total recall (R = 0.730, $p < .02$; Fig. 6). Receiver operating characteristic curves suggested that early changes in the cingula $\lambda_{||}$ predicted neurocognitive decline in the HVLT–total recall (Table 6). At 3 and 6 weeks after starting RT, the changes in the cingula $\lambda_{||}$ significantly predicted the decline in HVLT–total recall. Changes in cingula $\lambda_{||}$ at 30 weeks showed a trend toward prediction. However, the

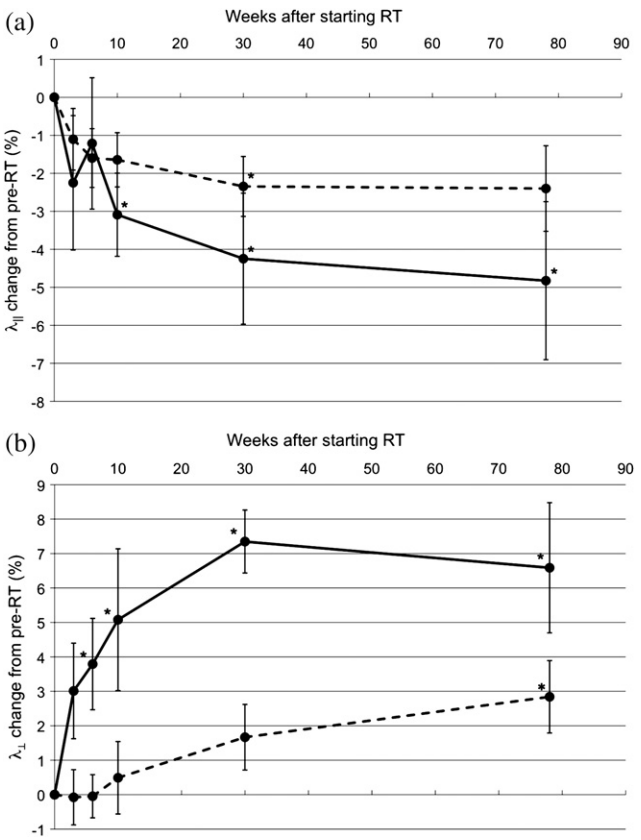

Fig. 2. (A) Changes in mean $\lambda_{||}$ over time. (B) Changes in mean $\lambda_{\perp}$ over time. Solid lines correspond to cingula, dashed lines to temporal lobe. Error bars indicate ± standard error. *Significant change from preradiotherapy values.

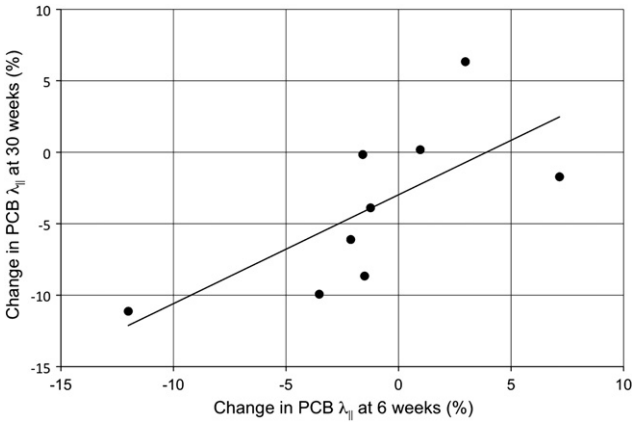

Fig. 3. Linear regression plot of percentage of change in cingula $\lambda_{||}$ at 6 weeks to percentage of change in cingula $\lambda_{||}$ at 30 weeks. Each dot represents 1 patient's cingula. R = 0.698, $p < .05$.

wide confidence intervals indicated that a larger study is needed to determine the actual predictive value of this measurement. Scores on the neurocognitive tests other than HVLT–total recall did not correlate with the DTI indexes. However, all 3 patients with late delayed decline in total recall also declined in the Controlled Oral Word Association, and 1 of the 3 had declines in HVLT–delayed recall. Changes in the cingula $\lambda_{\perp}$ and temporal lobe DTI indexes did not correlate with neurocognitive score changes.

We considered the relationship between radiation dose to the structures and neurocognitive function. The mean doses to the cingula, temporal lobe white matter, or hippocampi did not significantly relate to changes in the neurocognitive test scores. The $\%V_{12}$ of the structures was also not significantly related to changes in the neurocognitive test scores. This indicates that change in the cingula $\lambda_{||}$ was a better predictor of late delayed cognitive decline than the structure dose alone.

To determine the effect of cognitive decline on patients' quality of life, we studied the relationship between the neurocognitive test scores and EORTC QLQ-C30 and EORTC QLQ-BN20 survey results. Scores on the HVLT–total recall component and Trail Making Tests A and B correlated significantly with the quality-of-life survey scores ($p < .05$; Table 5). Scores on the HVLT–total recall component also correlated significantly with responses on the five questions chosen from the quality-of-life questionnaires to represent self-assessment of cognitive performance, at a greater significance threshold for post hoc analysis ($p < .01$; Table 5).

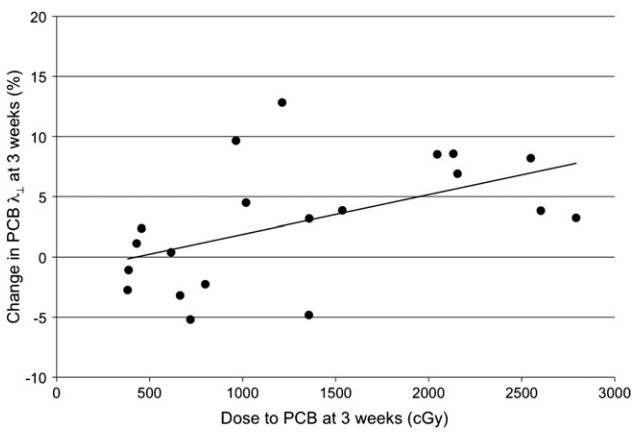

Fig. 4. Linear regression plots of percentage of change in cingulum $\lambda_{\perp}$ to dose at 3 weeks after starting radiotherapy. Each dot represents right or left cingulum in 1 patient. R = 0.493, $p < .05$.

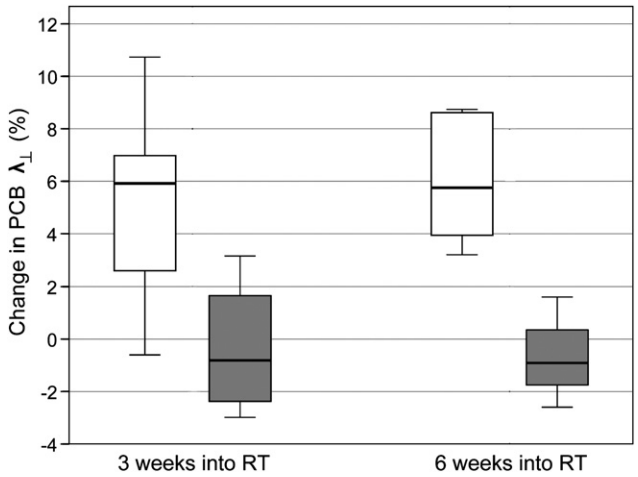

Fig. 5. Box plot showing range of percentage of change in cingula $\lambda_{\perp}$ at 3 and 6 weeks in patients with fraction of volume receiving ≥12 Gy >50% and <50% of cingula volume. Open box indicates fraction of volume receiving ≥12 Gy_2 >50% ($n = 6$); shaded box, fraction of volume receiving ≥12 Gy <50% ($n = 4$). Box represents 25th to 75th percentile, band indicates median, and whiskers, full range of values. Difference at 3 weeks, $p < .03$ and at 6 weeks, $p < .01$.

DISCUSSION

In the present study, we compared $\lambda_{||}$, an imaging biomarker of white matter axonal integrity, with neurocognitive function after cranial RT. Changes in cingula $\lambda_{||}$ at 30 weeks after starting RT correlated with the neurocognitive function changes. Also, decreases in cingula $\lambda_{||}$ at 3 and 6 weeks after starting RT were predictors for neurocognitive decline. Furthermore, changes in the cingula $\lambda_{||}$ at 6

Table 5. Neurocognitive scores

	Post-RT Z-score change			
	Mean	SD	Range	Neurocognitive decline (subjects/total)
HVLT-TR	−0.045	1.28	−2.63–1.35	3/9
HVLT-DR	−0.530	2.06	−5.88–1.11	2/9
COWA	−0.136	0.72	−1.02–1.42	5/9
TMT	0.738	1.62	−1.55–4.32	2/9

Abbreviations: RT = radiotherapy; SD = standard deviation; HVLT = hopkins verbal learning test; TR = total recall; DR = delayed recall; COWA = controlled oral word association; TMT = trail making test B – trail making test A.

Data presented as Z-scores normalized to age-based population data.

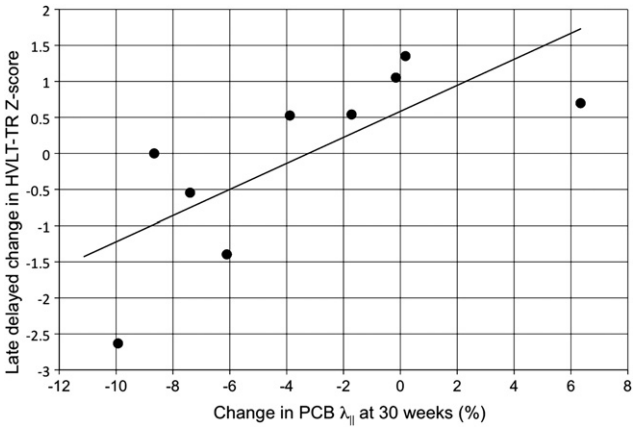

Fig. 6. Linear regression plot of percentage of change in cingula $\lambda_{||}$ at 30 weeks to Hopkins Verbal Learning Test total recall Z-score decrease. Each dot represents 1 patient's cingula. R = 0.730, $p < .02$.

weeks predicted additional changes in the cingula $\lambda_{||}$ at 30 weeks. These findings are consistent with our hypothesis that early white matter degradation eventually develops into injury substantial enough to cause late delayed cognitive decline. They also support our proposal that by identifying patients on a steeper early "trajectory" of white matter degradation, one might be able to predict which patients are at risk of radiation-induced neurocognitive decline. However, although a correlation was observed between the radiation dose and white matter diffusivity changes and between the diffusivity changes and neurocognitive function, the radiation dose to structures did not predict the neurocognitive function changes. This does not support the use of dose-sparing techniques to prevent neurocognitive decline. This might be because individual dose tolerances owing to genetic factors or other susceptibilities have a greater effect on neurocognitive decline risk, supported by the fact that in the general population, only 30–60% of patients receiving cranial radiation experience neurocognitive sequelae (2, 3). Also, the analysis of the mean dose and $\%V_{12}$ alone is an introductory approach, and a more complex study of normal tissue complication probability using a complete dose–volume histogram might reveal a dose-dependent interaction in a larger, more homogeneous, study population. Even if specific structures for dose sparing are not identified, this would not preclude the use of DTI as a biomarker for at-risk patients to receive prophylactic pharmaceutical or neuropsychological intervention; Gehring *et al.* (29) review the current research in these fields. Because none of our patients received chemotherapy, we are unable to determine how that might affect white matter injury or neurocognitive decline.

One consideration in the validity of our study was the effect of tumor progression itself on neurocognitive function changes. Meyers and Hess (30) have demonstrated that tumor progression is a risk factor for neurocognitive decline and that cognitive deterioration precedes progression by 6 weeks on average. However, continued clinical surveillance showed that no patient in our study had tumor progression <1 year after follow-up ended, implying that the observed cognitive decline was radiation induced and not due to tumor progression.

The observed post-RT decreases in $\lambda_{||}$ and increases in $\lambda_{\perp}$ are similar to previous observations of RT-induced white matter changes (12, 16). Although increases in vascular permeability might increase overall diffusion and reduce anisotropy (11), we believe that the changes observed were primarily due to white matter damage, because of the lack of increase in Dtr that would be expected if overall diffusion was increased after RT.

As a supplement to our major questions, we considered the clinical relevance of late delayed cognitive decline and found that scores on some neurocognitive function tests correlated with the quality-of-life survey results and to patients' self-assessment of cognition. This indicates that cognitive function changes as measured on standardized tests are substantial enough to cause appreciable detriment to quality of life. Patients' quality of life has been increasingly recognized as an important outcome in the treatment of central nervous system tumors (3). We propose that resources would, therefore, be well spent on understanding the causes, risk factors, and prevention of late delayed cognitive decline.

Future studies are intended to examine multiple white matter structures and to consider the effect of dose gradients within structures and the influence of the radiation field design. The results of the present study are encouraging for the development of DTI as a biomarker for radiation damage and late delayed cognitive decline. Our ultimate goal is to create better prediction metrics and improve the applicability for individual patients.

Table 6. Receiver operating characteristic of late delayed cognitive decline prediction by early changes in DTI indexes

	Hopkins Verbal Learning Total Recall				
Variable	AUC	95% CI	p	Max Acc	Cutoff (%)
Cingula $\lambda_{||}$ 3 wk	0.944	0.0–1.0	.039	0.889	−6.35
Cingula $\lambda_{||}$ 6 wk	1.00	1.0–1.0	.046	1.00	−1.86
Cingula $\lambda_{||}$ 30 wk	0.889	0.0–1.0	.071	0.889	−5.00

Abbreviations: DTI = diffusion tensor magnetic resonance imaging; AUC = area under curve; CI = confidence interval; p = asymptotic p value; Max Acc = maximal accuracy {[sensitivity × prevalence] + [specificity × (1 − prevalence)]}; Cutoff = cutoff value for maximal accuracy.

REFERENCES

1. Tofilon PJ, Fike JR. The radioresponse of the central nervous system: A dynamic process. *Radiat Res* 2000;153:357–370.
2. Crossen JR, Garwood D, Glatstein E, *et al*. Neurobehavioral sequelae of cranial irradiation in adults: A review of radiation-induced encephalopathy. *J Clin Oncol* 1994;12:627–642.
3. Meyers CA, Brown PD. Role and relevance of neurocognitive assessment in clinical trials of patients with CNS tumors. *J Clin Oncol* 2006;24:1305–1309.
4. Butler RW, Haser JK. Neurocognitive effects of treatment for childhood cancer. *Ment Retard Dev Disabil Res Rev* 2006;12: 184–191.
5. Chang EL, Wefel JS, Hess KR, *et al*. Neurocognition in patients with brain metastases treated with radiosurgery or radiosurgery plus whole-brain irradiation: A randomised controlled trial. *Lancet Oncol* 2009;10:1037–1044.
6. Wong CS, Van der Kogel AJ. Mechanisms of radiation injury to the central nervous system: Implications for neuroprotection. *Mol Interv* 2004;4:273–284.
7. Akiyama K, Tanaka R, Sato M, *et al*. Cognitive dysfunction and histological findings in adult rats one year after whole brain irradiation. *Neurol Med Chir (Tokyo)* 2001;41:590–598.
8. Khong P-L, Leung LHT, Fung ASM, *et al*. White matter anisotropy in post-treatment childhood cancer survivors: Preliminary evidence of association with neurocognitive function. *J Clin Oncol* 2006;24:884–890.
9. Mabbott DJ, Noseworthy MD, Bouffet E, *et al*. Diffusion tensor imaging of white matter after cranial radiation in children for medulloblastoma: Correlation with IQ. *Neuro-oncology* 2006; 8:244–252.
10. Mulhern RK, White HA, Glass JO, *et al*. Attentional functioning and white matter integrity among survivors of malignant brain tumors of childhood. *J Int Neuropsychol Soc* 2004;10: 180–189.
11. Assaf Y, Pasternak O. Diffusion tensor imaging (DTI)-based white matter mapping in brain research: A review. *J Mol Neurosci* 2008;34:51–61.
12. Haris M, Kumar S, Raj MK, *et al*. Serial diffusion tensor imaging to characterize radiation-induced changes in normal-appearing white matter following radiotherapy in patients with adult low-grade gliomas. *Radiat Med* 2008;26:140–150.
13. Nagesh V, Tsien CI, Chenevert TL, *et al*. Radiation-induced changes in normal-appearing white matter in patients with cerebral tumors: A diffusion tensor imaging study. *Int J Radiat Oncol Biol Phys* 2008;70:1002–1010.
14. Pierpaoli C, Basser PJ. Toward a quantitative assessment of diffusion anisotropy. *Magn Reson Med* 1996;36:893–906.
15. Song S-K, Sun S-W, Ju W-K, *et al*. Diffusion tensor imaging detects and differentiates axon and myelin degeneration in mouse optic nerve after retinal ischemia. *Neuroimage* 2003; 20:1714–1722.
16. Wang S, Wu EX, Qiu D, *et al*. Longitudinal diffusion tensor magnetic resonance imaging study of radiation-induced white matter damage in a rat model. *Cancer Res* 2009;69:1190–1198.
17. Ono J, Harada K, Takahashi M, *et al*. Differentiation between dysmyelination and demyelination using magnetic resonance diffusional anisotropy. *Brain Res* 1995;671:141–148.
18. Cao Y. Development of image software tools for radiation therapy assessment [Abstract]. *Med Phys* 2005;32(2136).
19. Chua TC, Wen W, Chen X, *et al*. Diffusion tensor imaging of the posterior cingulate is a useful biomarker of mild cognitive impairment. *Am J Geriatr Psychiatry* 2009;17:602–613.
20. Goldstein FC, Mao H, Wang L, *et al*. White matter integrity and episodic memory performance in mild cognitive impairment: A diffusion tensor imaging study. *Brain Imaging Behav* 2009;3: 132–141.
21. Lawrence YR, Li XA, el Naqa I, *et al*. Radiation dose–volume effects in the brain. *Int J Radiat Oncol Biol Phys* 2010;76(3 Suppl.):S20–S27.
22. Steel G. Basic clinical radiobiology. 3rd ed. London, UK: Arnold Publishers; 2002.
23. Benedict RHB, Schretlen D, Groninger L, *et al*. Hopkins Verbal Learning Test—Revised: Normative data and analysis of inter-form and test–retest reliability. *Clin Neuropsychol* 1998; 12:43–55.
24. Ruff RM, Light RH, Parker SB, *et al*. Benton Controlled Oral Word Association Test: Reliability and updated norms. *Arch Clin Neuropsychol* 1996;11:329–338.
25. Tombaugh TN. Trail Making Test A and B: Normative data stratified by age and education. *Arch Clin Neuropsychol* 2004;19:203–214.
26. Mehta MP, Shaprio WR, Phan SC, *et al*. Motexafin gadolinium combined with prompt whole brain radiotherapy prolongs time to neurologic progression in non–small-cell lung cancer patients with brain metastases: Results of a phase III trial. *Int J Radiat Oncol Biol Phys* 2009;73:1069–1076.
27. Aaronson N, Ahmedzai S, Bergman B, *et al*. The European Organization for Research and Treatment of Cancer QLQ-C30: A quality-of-life instrument for use in international clinical trials in oncology. *J Natl Cancer Inst* 1993;85:365–376.
28. Taphoorn MJB, Claassens L, Aaronson NK, *et al*. An international validation study of the EORTC brain cancer module (EORTC QLQ-BN20) for assessing health-related quality of life and symptoms in brain cancer patients. *Eur J Cancer* 2010;46:1033–1040.
29. Gehring K, Aaronson NK, Taphoorn MJ, *et al*. Interventions for cognitive deficits in patients with a brain tumor: An update. *Expert Rev Anticancer Ther* 2010;10:1779–1795.
30. Meyers CA, Hess KR. Multifaceted end points in brain tumor clinical trials: Cognitive deterioration precedes MRI progression. *Neuro-oncology* 2003;5:89–95.